JPE 9-2-7

Adaptive Flux Observer with On-line Inductance Estimation of an Interior PM Synchronous Machine Considering Magnetic Saturation

Yu-Seok Jeong† and Jun-Young Lee*

†*Dept. of Electrical Eng., Myongji University, Korea

ABSTRACT

This paper presents an adaptive flux observer to estimate stator flux linkage and stator inductances of an interior permanent-magnet synchronous machine considering magnetic saturation. The concept of static and dynamic inductances due to saturation is introduced in the machine model to describe the relationship between current and flux linkage and the relationship between their time derivatives. A flux observer designed in the stationary reference frame with constant inductance is analyzed in the rotor reference frame by a frequency-response characteristic. An adaptive algorithm for an on-line inductance estimation is proposed and a Lyapunov-based analysis is given to discuss its stability. The dynamic inductances are estimated by using Taylor approximation based on the static inductances estimated by the adaptive method. The simulation and experimental results show the feasibility and performance of the proposed technique.

Keywords: Adaptive flux observer, Magnetic saturation, Inductance estimation, Lyapunov-based analysis

1. Introduction

Interior permanent-magnet synchronous machines (IPM SMs) in automotive applications are typically designed to have a high saliency ratio under a wide range of operating conditions[1]. The magnetic characteristics of IPMSM are such that a lumped parameter model for these machines is nonlinear due to the saturated dq-axis inductances[2].

Based on the voltage equation of an IPMSM, its electrical system can be expressed as a dual-input-dual-output (DIDO) system, where the inputs and outputs are the stator voltages and the stator currents respectively. As parameters in this system, the stator resistance and the rotor-magnet flux linkage vary with temperature and the inductances vary with currents. The motor speed has been typically considered a slowly time-varying parameter rather than another state variable assuming that dynamics of the mechanical system is much slower than that of the electrical system.

Most research done on an observer in PMSM drive contribute to position estimation or load torque estimation in a sensorless control[3]-[5]. The stator inductances used in the flux observer are typically constants assuming no saturation, or are taken from two-dimensional (2D) look-up tables from motor characteristics to consider the saturation effect[6]. The estimated flux for sensorless control is processed to generate the position error in a position observer. With a position sensor, the flux observer can be used to estimate another machine's

Manuscript received June 23, 2008; revised Dec. 18, 2008
†Corresponding Author: jeong@mju.ac.kr
Tel: +82-31-330-6363, Fax: +82-31-321-0271, Myongji Univ.
*Dept. of Electrical Eng., Myongji University, Korea

parameters rather than the rotor position. Recently, an on-line inductance estimation scheme with a position sensor was introduced to improve the decoupling characteristics of a current controller designed in the rotor reference frame for an IPMSM drive[7]. This estimation technique is based on the voltage equation in a steady state and utilized the inverse of speed and current, which is not desirable when the machine operates at low speed or in light load.

This paper proposes an adaptive flux observer with on-line inductance estimation for an IPMSM with a position sensor. The flux observer is designed in the stationary reference frame rather than in the rotor reference frame to reduce the effect of inductance variation due to magnetic saturation on the estimation accuracy in steady state. The estimation error in the flux observer is transformed to that in the rotor reference frame and utilized to identify inductance variation in real time.

2. Mathematical Model of IPMSM Considering Magnetic Saturation

The flux linkage model of an IPMSM and its time derivative in the rotor reference frame can be generally written as

$$\boldsymbol{\lambda}^{\mathbf{r}}_{\mathbf{dq}} = \mathbf{L}_{\mathbf{s}}\mathbf{i}^{\mathbf{r}}_{\mathbf{dq}} + \boldsymbol{\Lambda}_{\mathbf{m}}, \quad \frac{d}{dt}\boldsymbol{\lambda}^{\mathbf{r}}_{\mathbf{dq}} = \mathbf{L}_{\mathbf{dq}}\frac{d}{dt}\mathbf{i}^{\mathbf{r}}_{\mathbf{dq}} \tag{1}$$

where $\boldsymbol{\lambda}^{\mathbf{r}}_{\mathbf{dq}}$ and $\mathbf{i}^{\mathbf{r}}_{\mathbf{dq}}$ denote the stator flux linkage vector and the stator current vector respectively. Static inductances, dynamic inductances and magnet flux linkage in (1) can be defined by

$$\mathbf{L}_{\mathbf{s}} = \begin{bmatrix} \dfrac{\lambda^r_d(i^r_d,0)-\lambda^r_d(0,0)}{i^r_d} & \dfrac{\lambda^r_d(i^r_d,i^r_q)-\lambda^r_d(i^r_d,0)}{i^r_q} \\ \dfrac{\lambda^r_q(i^r_d,i^r_q)-\lambda^r_q(0,i^r_q)}{i^r_d} & \dfrac{\lambda^r_q(0,i^r_q)-\lambda^r_q(0,0)}{i^r_q} \end{bmatrix},$$

$$\mathbf{L}_{\mathbf{dq}} = \begin{bmatrix} \dfrac{\partial\lambda^r_d}{\partial i^r_d} & \dfrac{\partial\lambda^r_d}{\partial i^r_q} \\ \dfrac{\partial\lambda^r_q}{\partial i^r_d} & \dfrac{\partial\lambda^r_q}{\partial i^r_q} \end{bmatrix}, \quad \boldsymbol{\Lambda}_{\mathbf{m}} = \begin{bmatrix} \lambda^r_d(0,0) \\ \lambda^r_q(0,0) \end{bmatrix} \tag{2}$$

The flux linkages of a test machine in this work with respect to the currents in the rotor reference frame are depicted in Fig. 1, where it can be seen that the saturation effect on the q-axis is more conspicuous than on the d-axis.

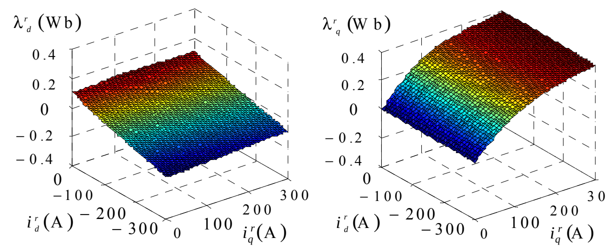

(a) (b)

Fig. 1 *d-q* flux linkage in the rotor reference frame
(a) d-axis flux linkage (b) q-axis flux linkage

Neglecting the cross magnetization unless the current is extremely high, the flux linkage only depends on the corresponding axis current in the rotor reference frame and the static and the dynamic inductances become diagonal.

$$\mathbf{L}_{\mathbf{s}} = \begin{bmatrix} L_{ds} & 0 \\ 0 & L_{qs} \end{bmatrix}, \quad \mathbf{L}_{\mathbf{dq}} = \begin{bmatrix} L_{dd} & 0 \\ 0 & L_{qq} \end{bmatrix} \tag{3}$$

where $L_{ds} = \dfrac{\lambda^r_d - \Lambda_m}{i^r_d}$, $L_{qs} = \dfrac{\lambda^r_q}{i^r_q}$, $L_{dd} = \dfrac{d\lambda^r_d}{di^r_d}$ and $L_{qq} = \dfrac{d\lambda^r_q}{di^r_q}$.

The stator voltage model of an IPMSM in the stationary reference frame can be expressed by

$$\mathbf{v}^{\mathbf{s}}_{\mathbf{dq}} = R_s\mathbf{i}^{\mathbf{s}}_{\mathbf{dq}} + \frac{d}{dt}\boldsymbol{\lambda}^{\mathbf{s}}_{\mathbf{dq}} \tag{4}$$

where R_s denotes the stator resistance.

The transformation between the stationary reference frame and the rotor reference frame can be expressed by the rotation matrix $\mathbf{R}(\theta_r) = \begin{bmatrix} \cos\theta_r & -\sin\theta_r \\ \sin\theta_r & \cos\theta_r \end{bmatrix}$.

3. Flux Observer

A flux observer designed in the stationary reference frame can be expressed by

$$\mathbf{v}_{\mathbf{dq}}^{\mathbf{s}} = \hat{R}_s\,\mathbf{i}_{\mathbf{dq}}^{\mathbf{s}} + \frac{d}{dt}\hat{\boldsymbol{\lambda}}_{\mathbf{dq}}^{\mathbf{s}} - \mathbf{K}_{\mathbf{o}}\left(\mathbf{i}_{\mathbf{dq}}^{\mathbf{s}} - \hat{\mathbf{i}}_{\mathbf{dq}}^{\mathbf{s}}\right) \tag{5}$$

where the circumflex denotes an estimated parameter/variable and $\mathbf{K}_{\mathbf{o}}$ denotes an observer gain matrix.

The observer block diagram is depicted in Fig. 2(a) and can be converted to its equivalent form in Fig. 2(b) by setting $\mathbf{K}_{\mathbf{o}} = \omega_o \mathbf{R}(\theta_r)\hat{\mathbf{L}}_{\mathbf{s}}\mathbf{R}^{-1}(\theta_r)$ as a time-varying gain. This yields

$$\begin{aligned}\mathbf{v}_{\mathbf{dq}}^{\mathbf{s}} &= \hat{R}_s\,\mathbf{i}_{\mathbf{dq}}^{\mathbf{s}} + \frac{d}{dt}\hat{\boldsymbol{\lambda}}_{\mathbf{dq}}^{\mathbf{s}} - \omega_o \mathbf{R}(\theta_r)\hat{\mathbf{L}}_{\mathbf{s}}\mathbf{R}^{-1}(\theta_r)\left(\mathbf{i}_{\mathbf{dq}}^{\mathbf{s}} - \hat{\mathbf{i}}_{\mathbf{dq}}^{\mathbf{s}}\right)\\ &= \hat{R}_s\,\mathbf{i}_{\mathbf{dq}}^{\mathbf{s}} + \frac{d}{dt}\hat{\boldsymbol{\lambda}}_{\mathbf{dq}}^{\mathbf{s}} - \omega_o \mathbf{R}(\theta_r)\hat{\mathbf{L}}_{\mathbf{s}}\left(\mathbf{i}_{\mathbf{dq}}^{\mathbf{r}} - \hat{\mathbf{i}}_{\mathbf{dq}}^{\mathbf{r}}\right)\\ &= \hat{R}_s\,\mathbf{i}_{\mathbf{dq}}^{\mathbf{s}} + \frac{d}{dt}\hat{\boldsymbol{\lambda}}_{\mathbf{dq}}^{\mathbf{s}} - \omega_o \mathbf{R}(\theta_r)\left\{\hat{\mathbf{L}}_{\mathbf{s}}\mathbf{R}^{-1}(\theta_r)\,\mathbf{i}_{\mathbf{dq}}^{\mathbf{s}} - \left(\hat{\boldsymbol{\lambda}}_{\mathbf{dq}}^{\mathbf{r}} - \hat{\boldsymbol{\Lambda}}_{\mathbf{m}}\right)\right\}\\ &= \hat{R}_s\,\mathbf{i}_{\mathbf{dq}}^{\mathbf{s}} + \frac{d}{dt}\hat{\boldsymbol{\lambda}}_{\mathbf{dq}}^{\mathbf{s}} - \omega_o\left[\mathbf{R}(\theta_r)\left\{\hat{\mathbf{L}}_{\mathbf{s}}\mathbf{R}^{-1}(\theta_r)\,\mathbf{i}_{\mathbf{dq}}^{\mathbf{s}} + \hat{\boldsymbol{\Lambda}}_{\mathbf{m}}\right\} - \hat{\boldsymbol{\lambda}}_{\mathbf{dq}}^{\mathbf{s}}\right]\end{aligned} \tag{6}$$

Defining two estimated fluxes, one is from a voltage model $\hat{\boldsymbol{\lambda}}_{\mathbf{v}}^{\mathbf{s}} = \int\left(\mathbf{v}_{\mathbf{dq}}^{\mathbf{s}} - \hat{R}_s\,\mathbf{i}_{\mathbf{dq}}^{\mathbf{s}}\right)dt$ and the other is from a current model $\hat{\boldsymbol{\lambda}}_{\mathbf{i}}^{\mathbf{s}} = \mathbf{R}(\theta_r)\left\{\hat{\mathbf{L}}_{\mathbf{s}}\mathbf{R}^{-1}(\theta_r)\,\mathbf{i}_{\mathbf{dq}}^{\mathbf{s}} + \hat{\boldsymbol{\Lambda}}_{\mathbf{m}}\right\}$. The closed-loop estimated flux with respect to these in a frequency domain can be expressed by

$$\hat{\boldsymbol{\lambda}}_{\mathbf{dq}}^{\mathbf{s}} = \frac{s}{s+\omega_o}\hat{\boldsymbol{\lambda}}_{\mathbf{v}}^{\mathbf{s}} + \frac{\omega_o}{s+\omega_o}\hat{\boldsymbol{\lambda}}_{\mathbf{i}}^{\mathbf{s}} \tag{7}$$

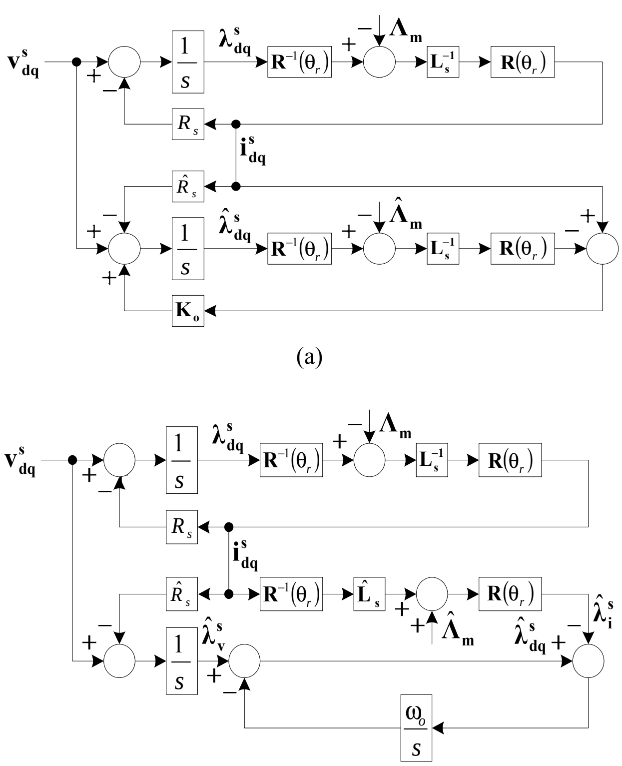

(a)

(b)

Fig. 2 Flux observer in the stationary reference frame
(a) original form (b) equivalent form

The estimated flux basically consists of the high-pass-filtered flux from the voltage model and the low-pass-filtered flux from the current model. Thus in steady state it follows the current model at low frequency and the voltage model at high frequency with the crossover frequency ω_o. Since this feature makes the flux observer robust to inductance variation at high frequency, the flux observer is preferred to be designed in the stationary reference frame rather than in the rotor reference frame[8].

Even though the flux observer is designed in the stationary reference frame, its dynamic characteristics in a frequency domain can be analyzed in the rotor reference frame. Transforming (4) and (6) to the rotor reference frame and applying the Laplace transform yields

$$\begin{aligned}\hat{\boldsymbol{\lambda}}_{\mathbf{dq}}^{\mathbf{r}} &= \left(s\mathbf{I} + \omega_r\mathbf{J} + \omega_o\mathbf{I}\right)^{-1}\\ &\times\Big[\left\{s\mathbf{I} + \omega_r\mathbf{J} + \left(R_s\mathbf{I} - \hat{R}_s\mathbf{I} + \omega_o\hat{\mathbf{L}}_{\mathbf{s}}\right)\mathbf{L}_{\mathbf{s}}^{-1}\right\}\boldsymbol{\lambda}_{\mathbf{dq}}^{\mathbf{r}}\\ &\quad - \left(R_s\mathbf{I} - \hat{R}_s\mathbf{I} + \omega_o\hat{\mathbf{L}}_{\mathbf{s}}\right)\mathbf{L}_{\mathbf{s}}^{-1}\boldsymbol{\Lambda}_{\mathbf{m}} + \omega_o\hat{\boldsymbol{\Lambda}}_{\mathbf{m}}\Big]\end{aligned} \tag{8}$$

where $\mathbf{J} = \begin{bmatrix} 0 & -1 \\ 1 & 0 \end{bmatrix}$.

It can be seen that the transfer matrix becomes the unity without parameter variation.

The steady-state characteristic of the flux observer can also be analyzed by using complex vector notations. Substituting $s = 0$ and in (8) and using the relationship $\Lambda_d^r = 0.5\left(\Lambda_{dq}^r + \overline{\Lambda}_{dq}^r\right)$ and $\Lambda_q^r = -j0.5\left(\Lambda_{dq}^r - \overline{\Lambda}_{dq}^r\right)$ to obtain complex vector expression yields

$$\hat{\Lambda}_{dq}^r = G_\lambda(j\omega_r)\Lambda_{dq}^r + G_{\overline{\lambda}}(j\omega_r)\overline{\Lambda}_{dq}^r + G_\Lambda(j\omega_r)\Lambda_m$$

$$G_\lambda(j\omega_r) = \frac{\frac{R_s}{2}\left(1 - \frac{\hat{R}_s}{R_s}\right)\left(\frac{1}{L_{ds}} + \frac{1}{L_{qs}}\right) + \frac{\omega_o}{2}\left(\frac{\hat{L}_{ds}}{L_{ds}} + \frac{\hat{L}_{qs}}{L_{qs}}\right) + j\omega_r}{\omega_o + j\omega_r}$$

$$G_{\bar{\lambda}}(j\omega_r)=\frac{\dfrac{R_s}{2}\left(1-\dfrac{\hat{R}_s}{R_s}\right)\left(\dfrac{1}{L_{ds}}-\dfrac{1}{L_{qs}}\right)+\dfrac{\omega_o}{2}\left(\dfrac{\hat{L}_{ds}}{L_{ds}}-\dfrac{\hat{L}_{qs}}{L_{qs}}\right)}{\omega_o+j\omega_r}$$

$$G_{\Lambda}(j\omega_r)=-\frac{\dfrac{R_s}{L_{ds}}\left(1-\dfrac{\hat{R}_s}{R_s}\right)+\omega_o\left(\dfrac{\hat{L}_{ds}}{L_{ds}}-\dfrac{\hat{\Lambda}_m}{\Lambda_m}\right)}{\omega_o+j\omega_r} \tag{9}$$

where $\hat{\Lambda}_{dq}^r$, Λ_{dq}^r and $\bar{\Lambda}_{dq}^r$ denote the estimated flux vector, the actual flux vector, and the conjugate flux vector in steady state, respectively. It should be noted that the conjugate expression comes from the inherent saliency of an IPMSM. The geometric interpretation of (9) in the DQ plane is shown in Fig. 3.

The sensitivity of the flux observer to parameter variation can be analyzed from the transfer matrix in (8).

$$\begin{aligned}
\mathbf{S}_{R_s} &= R_s\{(s+\omega_o)\mathbf{I}+\omega_r\mathbf{J}\}^{-1}\mathbf{L}_s^{-1}\\
\mathbf{S}_{L_{ds}} &= L_{ds}\{(s+\omega_o)\mathbf{I}+\omega_r\mathbf{J}\}^{-1}\omega_o\mathbf{L}_s\frac{\partial}{\partial L_{ds}}\mathbf{L}_s^{-1}\\
\mathbf{S}_{L_{qs}} &= L_{qs}\{(s+\omega_o)\mathbf{I}+\omega_r\mathbf{J}\}^{-1}\omega_o\mathbf{L}_s\frac{\partial}{\partial L_{qs}}\mathbf{L}_s^{-1}
\end{aligned} \tag{10}$$

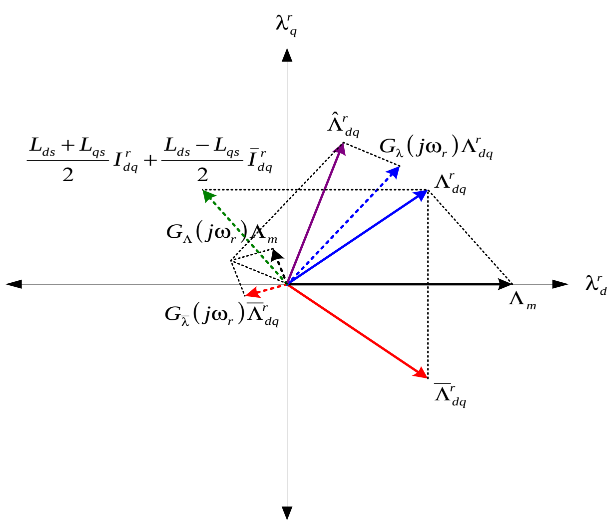

Fig. 3 Estimated steady-state flux vector

While the sensitivity in a single-input-single-output (SISO) system is typically analyzed using the magnitude of the transfer function, it is analyzed using the matrix norm of the transfer matrix in a multi-input-multi-output (MIMO) system.

$$\begin{aligned}
\left\|\mathbf{S}_{R_s}\right\| &= \sigma_{\max}\left[\mathbf{S}_{R_s}(j\omega)\right]=\sqrt{\lambda_{\max}\left[\mathbf{S}_{R_s}^{\mathrm{T}}(-j\omega)\mathbf{S}_{R_s}(j\omega)\right]}\\
\left\|\mathbf{S}_{L_{ds}}\right\| &= \sigma_{\max}\left[\mathbf{S}_{L_{ds}}(j\omega)\right]=\sqrt{\lambda_{\max}\left[\mathbf{S}_{L_{ds}}^{\mathrm{T}}(-j\omega)\mathbf{S}_{L_{ds}}(j\omega)\right]}\\
\left\|\mathbf{S}_{L_{qs}}\right\| &= \sigma_{\max}\left[\mathbf{S}_{L_{qs}}(j\omega)\right]=\sqrt{\lambda_{\max}\left[\mathbf{S}_{L_{qs}}^{\mathrm{T}}(-j\omega)\mathbf{S}_{L_{qs}}(j\omega)\right]}
\end{aligned} \tag{11}$$

where $\sigma_{\max}[\cdot]$ and $\lambda_{\max}[\cdot]$ denote the maximum singular value and the maximum eigenvalue, respectively.

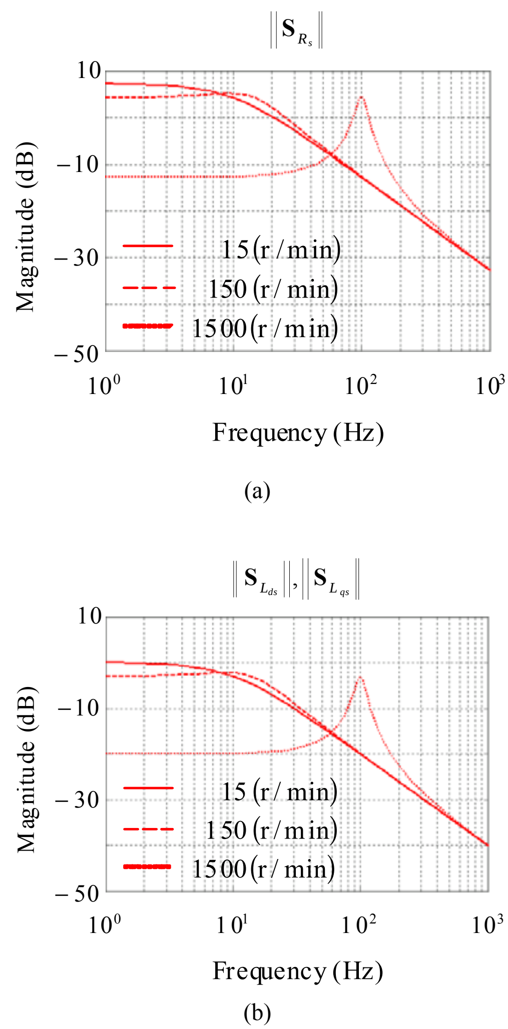

Fig. 4 Sensitivity of the flux observer to parameter variation (a) resistance sensitivity (b) inductance sensitivity

For the test motor with its parameters in Table 1, the sensitivity of the flux observer to parameter variation with the crossover frequency $\omega_o = 20\pi$ rad/sec is depicted in Fig. 4. The resistance sensitivity is shown in Fig. 4(a) and is almost constant below the crossover frequency, reaches its peak at the operating frequency and is declined as the frequency increases. This feature depending on the operating speed is based on the transformation between the reference frames. The inductance sensitivity is shown in Fig. 4(b) and is similar to the resistance sensitivity. A decrease of the sensitivity to parameter variation at a high operating speed is due to a lesser effect on the estimated flux from the open-loop voltage model. It should be noted that increasing the order of the transfer matrix results in less sensitivity to resistance variation at low operating speed but more sensitivity to inductance variation at high operating speed[9].

4. Inductance Estimation

The static inductance can be estimated by using the estimation error transformed to the rotor reference frame. The error dynamics of the flux observer can be derived from (4) and (6).

$$\frac{d}{dt}\Delta\boldsymbol{\lambda}^{s}_{\mathbf{dq}} = -\omega_o\Delta\boldsymbol{\lambda}^{s}_{\mathbf{dq}} + \omega_o\mathbf{R}(\theta_r)\Delta\mathbf{L_s}\mathbf{R}^{-1}(\theta_r)\,\mathbf{i}^{s}_{\mathbf{dq}} - \Delta R_s\mathbf{i}^{s}_{\mathbf{dq}} + \omega_o\mathbf{R}(\theta_r)\Delta\boldsymbol{\Lambda}_{\mathbf{m}} \tag{12}$$

where $\Delta\boldsymbol{\lambda}^{s}_{\mathbf{dq}} = \boldsymbol{\lambda}^{s}_{\mathbf{dq}} - \hat{\boldsymbol{\lambda}}^{s}_{\mathbf{dq}}$, $\Delta R_s = R_s - \hat{R}_s$, $\Delta\mathbf{L_s} = \mathbf{L_s} - \hat{\mathbf{L}}_{\mathbf{s}}$, and $\Delta\boldsymbol{\Lambda}_{\mathbf{m}} = \boldsymbol{\Lambda}_{\mathbf{m}} - \hat{\boldsymbol{\Lambda}}_{\mathbf{m}}$. In the left side of (12), the 1st term is related to the state variable, the 2nd term to input, and other terms is treated as disturbance.

A positive definite function can be defined by

$$V = \Delta\boldsymbol{\lambda}^{s\,\mathrm{T}}_{\mathbf{dq}}\Delta\boldsymbol{\lambda}^{s}_{\mathbf{dq}} + \omega_o\, tr\left(\Delta\mathbf{L_s}^{\mathrm{T}}\boldsymbol{\Gamma}^{-1}\Delta\mathbf{L_s}\right) \tag{13}$$

where tr denotes a trace of a matrix, and this function becomes a Lyapunov-like function since the input variable in (12), i.e. the current is another state variable to be controlled.

An input coefficient in the error dynamics is typically estimated by the multiplication of estimation error and input[10]. It should be noted that the estimation error of the current should be used since that of the flux linkage is not available. Therefore the adaptive law for inductance estimation can be described by

$$\begin{aligned}\frac{d}{dt}\Delta\mathbf{L}_s &= \boldsymbol{\Gamma}\,\hat{\mathbf{L}}_s\,\mathbf{R}^{-1}(\theta_r)\left(\mathbf{i}^{s}_{\mathbf{dq}} - \hat{\mathbf{i}}^{s}_{\mathbf{dq}}\right)\mathbf{i}^{s\,\mathrm{T}}_{\mathbf{dq}}\,\mathbf{R}(\theta_r)\\ &= \boldsymbol{\Gamma}\left\{\hat{\boldsymbol{\lambda}}^{r}_{\mathbf{dq}} - \left(\hat{\mathbf{L}}_s\mathbf{i}^{r}_{\mathbf{dq}} + \hat{\boldsymbol{\Lambda}}_{\mathbf{m}}\right)\right\}\mathbf{i}^{r\,\mathrm{T}}_{\mathbf{dq}}\\ &= \boldsymbol{\Gamma}\left(\Delta\boldsymbol{\lambda}^{r}_{\mathbf{dq}} - \Delta\mathbf{L}_s\mathbf{i}^{r}_{\mathbf{dq}} - \Delta\boldsymbol{\Lambda}_{\mathbf{m}}\right)\mathbf{i}^{r\,\mathrm{T}}_{\mathbf{dq}}\end{aligned} \tag{14}$$

where $\boldsymbol{\Gamma}$ denotes the adaptive gain matrix. It can be seen that the static inductances are estimated using the variables in the rotor reference frame. To check the stability of this adaptive technique, differentiating (13) yields.

$$\begin{aligned}\frac{dV}{dt} &= \left(\frac{d}{dt}\Delta\boldsymbol{\lambda}^{s}_{\mathbf{dq}}\right)^{\mathrm{T}}\Delta\boldsymbol{\lambda}^{s}_{\mathbf{dq}} + \Delta\boldsymbol{\lambda}^{s\,\mathrm{T}}_{\mathbf{dq}}\left(\frac{d}{dt}\Delta\boldsymbol{\lambda}^{s}_{\mathbf{dq}}\right)\\ &\quad + \omega_o\, tr\left\{\left(\frac{d}{dt}\Delta\mathbf{L}_s\right)^{\mathrm{T}}\boldsymbol{\Gamma}^{-1}\Delta\mathbf{L}_s + \Delta\mathbf{L}_s^{\mathrm{T}}\boldsymbol{\Gamma}^{-1}\left(\frac{d}{dt}\Delta\mathbf{L}_s\right)\right\}\\ &= -2\omega_o\left(\Delta\boldsymbol{\lambda}^{r}_{\mathbf{dq}} - \Delta\mathbf{L}_s\mathbf{i}^{r}_{\mathbf{dq}}\right)^{\mathrm{T}}\left(\Delta\boldsymbol{\lambda}^{r}_{\mathbf{dq}} - \Delta\mathbf{L}_s\mathbf{i}^{r}_{\mathbf{dq}}\right)\\ &\quad - \Delta R_s\left(\mathbf{i}^{r\,\mathrm{T}}_{\mathbf{dq}}\Delta\boldsymbol{\lambda}^{r}_{\mathbf{dq}} + \Delta\boldsymbol{\lambda}^{r\,\mathrm{T}}_{\mathbf{dq}}\mathbf{i}^{r}_{\mathbf{dq}}\right)\\ &\quad + \omega_o\left\{\left(\Delta\boldsymbol{\lambda}^{r}_{\mathbf{dq}} - \Delta\mathbf{L}_s\mathbf{i}^{r}_{\mathbf{dq}}\right)^{\mathrm{T}}\Delta\boldsymbol{\Lambda}_{\mathbf{m}}\right.\\ &\quad \left. + \Delta\boldsymbol{\Lambda}_{\mathbf{m}}^{\mathrm{T}}\left(\Delta\boldsymbol{\lambda}^{r}_{\mathbf{dq}} - \Delta\mathbf{L}_s\mathbf{i}^{r}_{\mathbf{dq}}\right)\right\}\end{aligned} \tag{15}$$

The time derivative of the Lyapunov-like function in (13) does not become positive with actual values of the stator resistance and the rotor magnet flux linkage, which is hardly achievable. To prevent undesirable blow-up, the projection method is utilized to estimate inductances with an adaptive technique.

$$\begin{aligned}&if\ \hat{L}_{ds} < L_{do}\ or\ \hat{L}_{ds} = L_{do},\ i^r_d\left(\hat{\lambda}^r_d - \hat{\Lambda}_m - \hat{L}_{ds}i^r_d\right) \le 0\\ &\qquad \frac{d}{dt}\hat{L}_{ds} = \gamma_d\, i^r_d\left(\hat{\lambda}^r_d - \hat{\Lambda}_m - \hat{L}_{ds}i^r_d\right)\\ &otherwise\ \ \frac{d}{dt}\hat{L}_{ds} = 0\\ &if\ \hat{L}_{qs} < L_{qo}\ or\ \hat{L}_{qs} = L_{qo},\ i^r_q\left(\hat{\lambda}^r_q - \hat{L}_{qs}i^r_q\right) \le 0\\ &\qquad \frac{d}{dt}\hat{L}_{qs} = \gamma_q\, i^r_q\left(\hat{\lambda}^r_q - \hat{L}_{qs}i^r_q\right)\\ &otherwise\ \ \frac{d}{dt}\hat{L}_{qs} = 0\end{aligned} \tag{16}$$

The adaptive flux observer with on-line inductance esti-

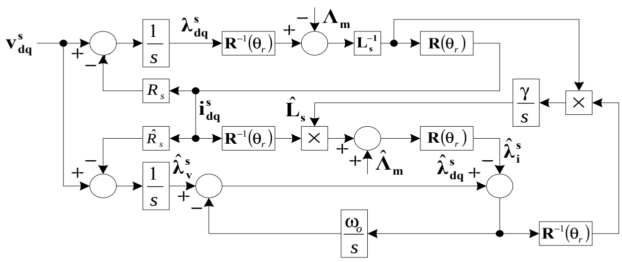
Fig. 5 On-line inductance estimation

mation is depicted in Fig. 5. The estimated inductance which is constant in the previous flux observer is now updated in real time. It is crucial to check the condition for persistent excitation when an adaptive scheme is used.

Dynamic inductances are defined by the relationship between the time derivatives of current and flux linkage in the rotor reference frame. Therefore it is impossible to estimate dynamic inductances in steady state using the definition in (1). An estimation method using Taylor approximation of flux linkage is developed.

$$\boldsymbol{\lambda}_{\mathbf{dq}}^{\mathbf{r}}\left(\mathbf{i}_{\mathbf{dq}}^{\mathbf{r}}\right)=\begin{bmatrix}\lambda_d^r(0,0)\\ \lambda_q^r(0,0)\end{bmatrix}+\begin{bmatrix}\mathbf{i}_{\mathbf{dq}}^{\mathbf{r}\,T}\,\nabla\lambda_d^r(0,0)\\ \mathbf{i}_{\mathbf{dq}}^{\mathbf{r}\,T}\,\nabla\lambda_q^r(0,0)\end{bmatrix}+\frac{1}{2}\begin{bmatrix}\mathbf{i}_{\mathbf{dq}}^{\mathbf{r}\,T}\,\nabla^2\lambda_d^r(0,0)\,\mathbf{i}_{\mathbf{dq}}^{\mathbf{r}}\\ \mathbf{i}_{\mathbf{dq}}^{\mathbf{r}\,T}\,\nabla^2\lambda_q^r(0,0)\,\mathbf{i}_{\mathbf{dq}}^{\mathbf{r}}\end{bmatrix}+\cdots \tag{17}$$

Neglecting cross magnetization and using the definition of inductances in (3), the dynamic inductance can be estimated from the static inductance.

$$\hat{\mathbf{L}}_{\mathbf{dq}} \approx \begin{bmatrix}\frac{d\lambda_d^r}{di_d^r}(0) & 0\\ 0 & \frac{d\lambda_q^r}{di_q^r}(0)\end{bmatrix}^{-1}\hat{\mathbf{L}}_{\mathbf{s}}^2 \tag{18}$$

5. Simulation and Experiment

The adaptive flux observer with on-line inductance estimation has been investigated by computer simulations and lab experiments. Simulink® was used for the computer simulation. The IPMSM used in this simulation and experiment is an integrated starter/alternator for automotive applications.

Table 1 Nominal machine parameters

Symbol	Description	Value (Unit)
P_{rated}	Rated Power	5 (kW)
V_{rated}	Rated Voltage	30 (Vrms)
I_{rated}	Rated Current	150 (Arms)
P	Pole pairs	4 (n.u.)
R_s	Stator resistance	13 (mΩ)
L_{ds}	D-axis inductance	90 (μH)
L_{qs}	Q-axis inductance	290 (μH)
Λ_m	Magnet flux linkage	11 (mV·sec)

The nominal parameters of this machine are shown in Table 1. The test condition is the torque command of 30 Nm at three different speeds of 15 r/min, 150 r/min, and 1500 r/min which correspond to 1 Hz, 10 Hz, and 100 Hz, respectively. The crossover frequency of the flux observer is set to 20π rad/sec which corresponds to 10 Hz.

The simulation result for the flux observer without inductance estimation is depicted in Fig. 6. The upper figures in (a), (b), and (c) show the calculated flux from the look-up table and the estimated flux from the flux observer on d-axis. The lower figures show those on q-axis. The estimation accuracy at low speed shown in (a) is worse on q-axis, since magnetic saturation makes more of an effect on q-axis. The estimation accuracy at the crossover frequency shown in (b) becomes better on q-axis, but worse on d-axis since it has the most cross-coupling effect at this speed. The estimation accuracy at high speed shown in (c) becomes better on both axes since the flux is estimated dominantly from the voltage model, which takes no effect from inductance variation. The characteristic of the flux observer with inductance estimation is depicted in Fig. 7. The estimation accuracy is improved particularly at low speed. The inductance estimation using the proposed adaptive law is shown in Fig. 8.

The test setup employs a TI's DSP-based controller with the sampling time of 0.1ms for the current control. The experiments under the same condition are depicted for the flux observer without inductance estimation in Fig. 9, for the flux observer with inductance estimation in Fig. 10, and for the inductance estimation by the adaptive law in Fig. 11. It matches well with the simulation results, except for periodic ripples at high speed. These ripples having operating frequency are caused from the periodic position errors in synchronization with the rotation cycle of the resolver that occur due to its structure[11].

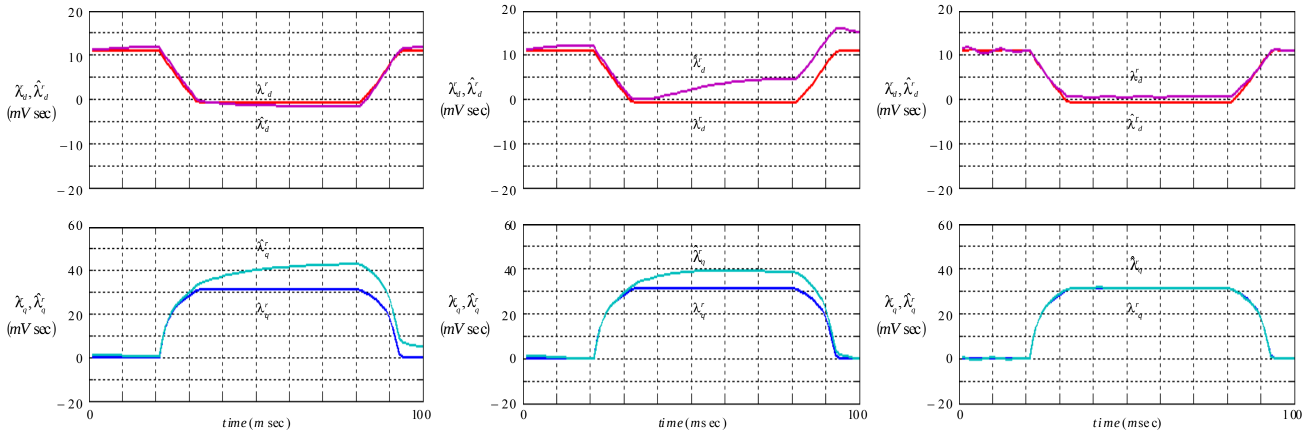

(a) (b) (c)

Fig. 6 Estimation characteristics of the flux observer without inductance estimation (simulation)

(a) 30 Nm command at 15 r/min (b) 30 Nm command at 150 r/min (c) 30 Nm command at 1500 r/min

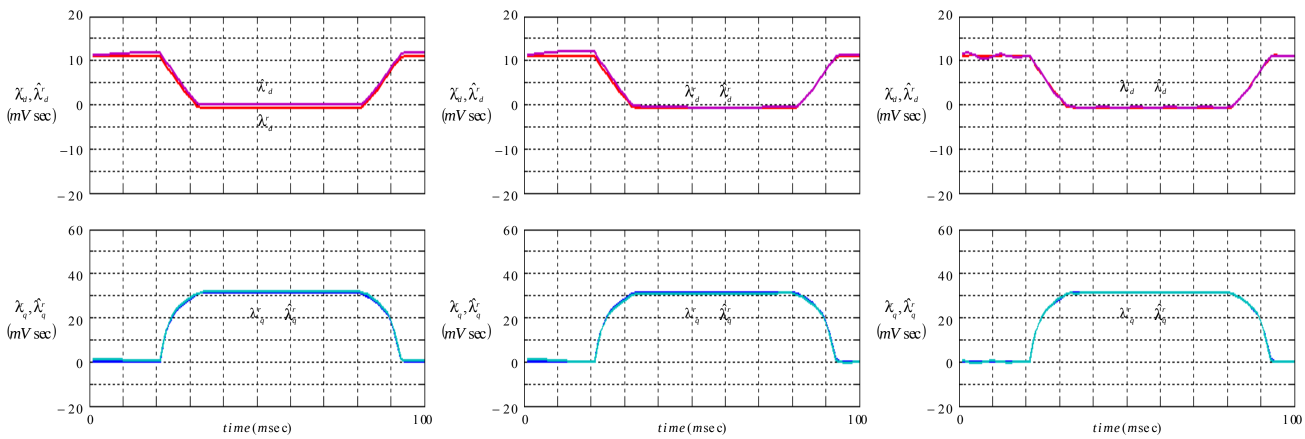

(a) (b) (c)

Fig. 7 Estimation characteristics of the flux observer with inductance estimation (simulation)

(a) 30 Nm command at 15 r/min (b) 30 Nm command at 150 r/min (c) 30 Nm command at 1500 r/min

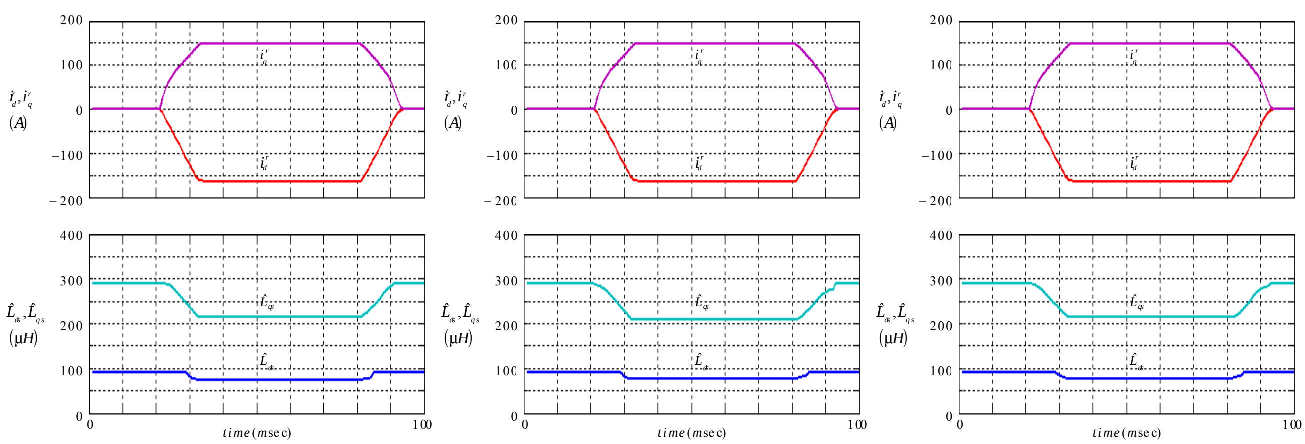

(a) (b) (c)

Fig. 8 On-line inductance estimation using the proposed adaptive method (simulation)

(a) 30 Nm command at 15 r/min (b) 30 Nm command at 150 r/min (c) 30 Nm command at 1500 r/min

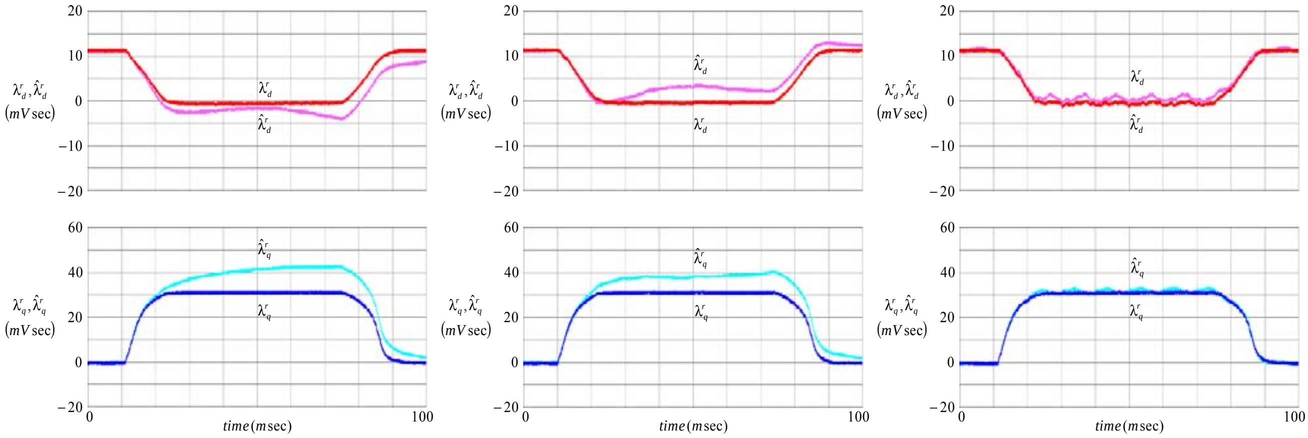

(a) (b) (c)

Fig. 9 Estimation characteristics of the flux observer without inductance estimation (experiment)

(a) 30 Nm command at 15 r/min (b) 30 Nm command at 150 r/min (c) 30 Nm command at 1500 r/min

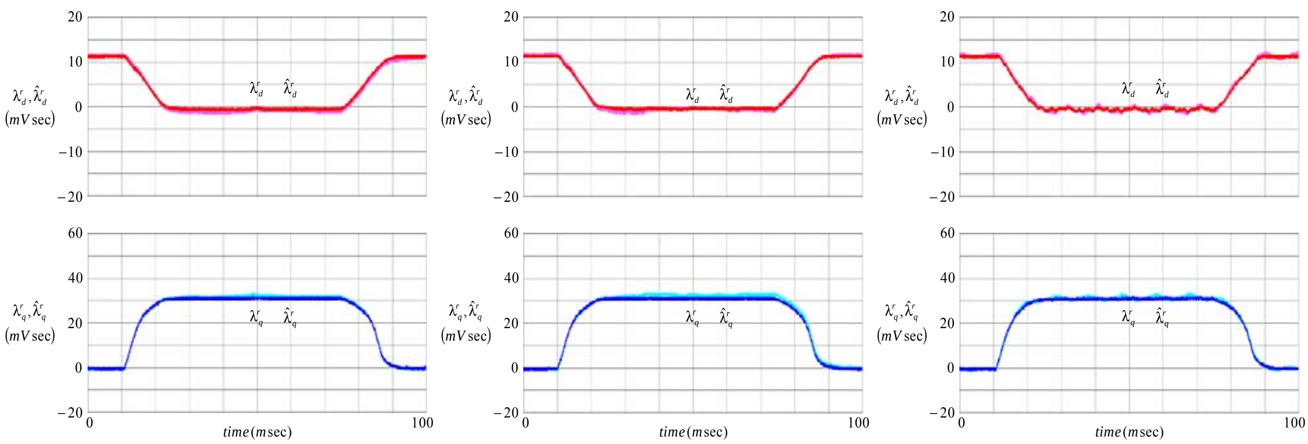

(a) (b) (c)

Fig. 10 Estimation characteristics of the flux observer with inductance estimation (experiment)

(a) 30 Nm command at 15 r/min (b) 30 Nm command at 150 r/min (c) 30 Nm command at 1500 r/min

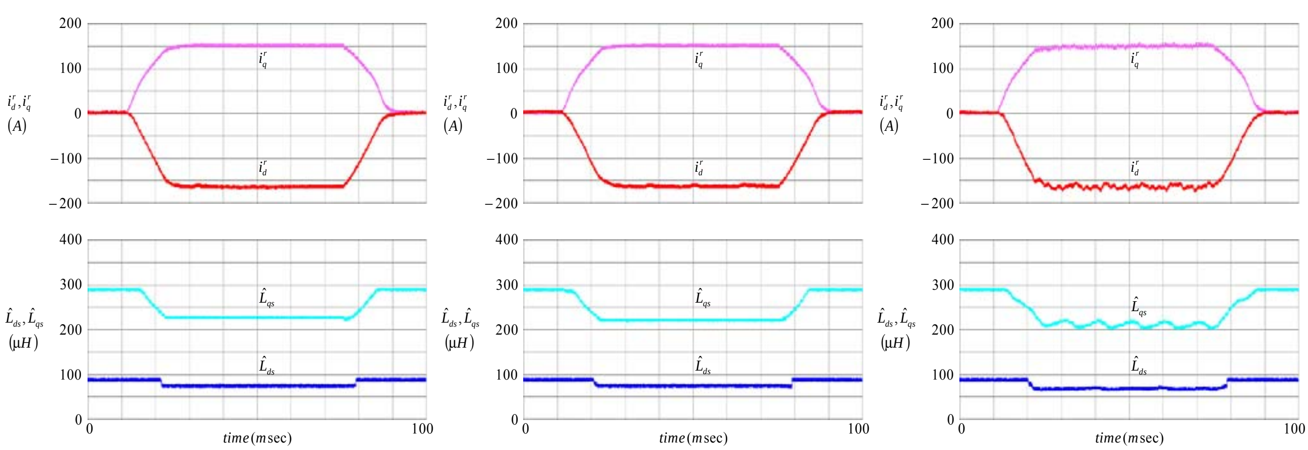

(a) (b) (c)

Fig. 11 On-line inductance estimation using the proposed adaptive method (experiment)

(a) 30 Nm command at 15 r/min (b) 30 Nm command at 150 r/min (c) 30 Nm command at 1500 r/min

6. Conclusions

The paper has introduced an adaptive flux observer with on-line inductance estimation for an IPMSM considering magnetic saliency. The flux observer is designed in the stationary reference frame to be robust to inductance variation at high speed in steady state and the estimation error of the flux observer is transformed to the rotor reference frame and utilized to estimate static inductances. Dynamic inductance is estimated from static inductance by Taylor approximation. The simulation and experiment results have demonstrated that this technique is effective at an overall operating frequency. Even at very low speed, the estimation accuracy is well maintained as long as a transient occurs fast enough to utilize the voltage information. Further work on cross magnetization and magnet flux variation due to temperature can be helpful to extend this research.

Acknowledgment

This work was financially supported by the advanced human resource development program of MKE (Ministry of Knowledge and Economy) through the Research Center for Intelligent Microgrid in Myongji University.

References

[1] E. C. Lovelace, T. M. Jahns, J. L. Kirtley and J. H. Lang, "An interior PM starter/alternator for automotive applications", *in Proc. ICEM.*, Vol. 3, No. 3, pp.1802-1808, 1998.

[2] E. C. Lovelace, T. M. Jahns, and J. H. Lang, "A saturating lumped-parameter model for an interior PM synchronous machine", *IEEE Trans. Industry Applications*, Vol. 38, pp. 645-650, May/June 2002.

[3] Z. Chen, M. Tomita, S. Doki, and S. Okuma, "New adaptive sliding observers for position- and velocity-sensorless controls of brushless DC motors", *IEEE Trans. Industrial Electronics*, Vol. 47, pp. 582-591, June 2000.

[4] P. Gaur, B. Singh, and A. P. Mittal, "Steady state and dynamic response of a state space observer based PMSM drive with different controllers", *Journal of Power Electronics*, Vol. 8, No. 3, pp. 280-290, 2008.

[5] J. Ko, Y. Seo, and H. Kim, "Precision position control of PMSM using neural observer and parameter compensator", *Journal of Power Electronics*, Vol. 8, No. 4, pp. 354-362, 2008.

[6] P. Guglielmi, M. Pastorelli, G. Pellegrino and A. Vagati, "Position-sensorless control of permanent-magnet-assisted synchronous reluctance motor", *IEEE Trans. Industry Applications*, Vol. 40, pp. 615-622, Mar./Apr. 2004.

[7] H. Kim and R. D. Lorenz, "Improved current regulators for IPM machine drives using on-line parameter estimation", *IEEE IAS annual meeting*, Vol. 1, pp. 86-91, 2002.

[8] P. L. Jansen and R. D. Lorenz, "A physically insightful approach to the design and accuracy assessment of flux observers for field oriented induction machine drives", *IEEE Trans. Industry Applications*, Vol. 30, pp. 101-110, Jan./Feb. 1994.

[9] Y. Jeong, "On-line minimum-copper-loss control of a permanent- magnet synchronous machine considering magnetic saturation", Ph. D. dissertation, Seoul National University, 2005.

[10] P. A. Ioannou and J. Sun, *Robust Adaptive Control*. New Jersey: Prentice Hall, ch. 4, 1996.

[11] H. Yaguchi and S. Sasaki, "The motor control technologies for high-power hybrid system", *SAE Technical paper series*, 2005.

Yu-Seok Jeong was born in Daegu, Korea, in 1971. He received his B.S., M.S. and Ph.D. degrees from Seoul National University, Seoul, Korea, in 1993, 1995, and 2005, respectively, all in Electrical Engineering. He joined the Kia Motors Technical Center, Seoul, Korea, as a Research Engineer in 1995. In 2001 and 2002, he was a special student at the University of Wisconsin, Madison. During his doctoral course, he pursued fault-tolerant control and robust adaptive control of IPM synchronous machine drives in collaboration with GM. Following a one-year experience to develop a motor drive system for HEV/FCV applications at Hyundai Motor Company in 2005, he is currently with the Dept. of Electrical Eng., Myongji Univ., Gyeonggi-do, Korea. His research interests include modeling and digital control of power electronics and energy conversion.

Jun-Young Lee was born in Seoul, Korea in 1970. He received his B.S. degree in Electrical Engineering from Korea University, Seoul, in 1993 and his M.S. and Ph.D. degrees in Electrical Engineering from Korea Advanced Institute of Science and Technology, Taejon, Korea, in 1996 and 2001, respectively. From 2001 to 2005, he worked as a Manager in Plasma Display Panel Development Group, Samsung SDI where he was involved in circuit and product development. From 2005 to 2008, he worked as a faculty member in the School of Electronics and Computer Engineering, Dankook University, Chungnam, Korea. In 2008, he joined the Department of Electrical Engineering, Myongji University, Gyeonggi-do, Korea, as an assistant professor. His research interests are in the areas of power electronics which include AC/DC power factor correction converter topology design, converter modeling, soft switching techniques, display driving system, and liquid crystal display backlight units. Dr. Lee is a member of the Korea Institute of Electrical Engineering (KIEE), Korea Institute of Power Electronics (KIPE), and the IEEE Industrial Electronics and IEEE Power Electronics Societies.